Electronic Supplementary Material (ESI) for RSC Advances.

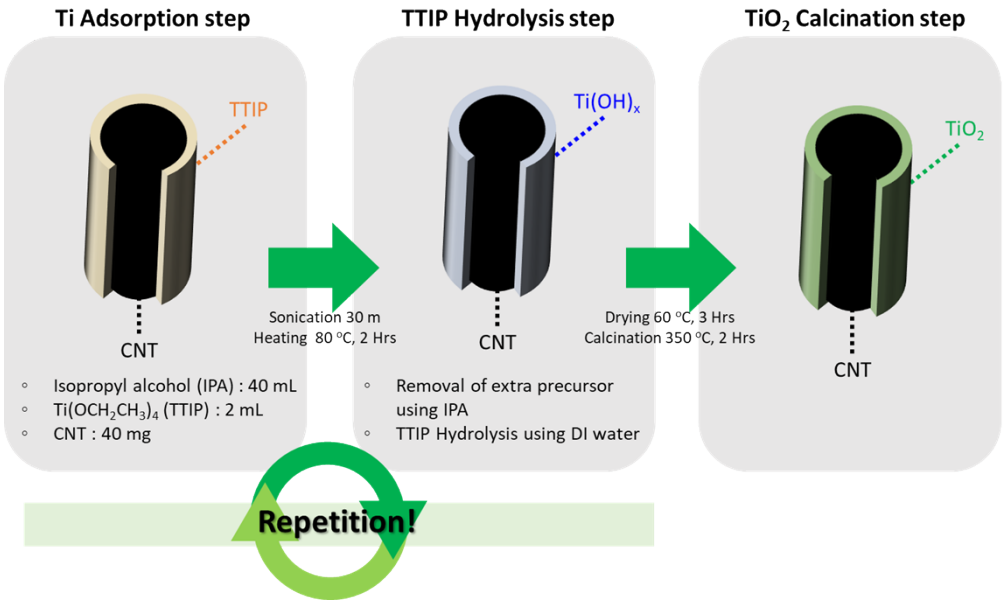

Figure S1. A schematic illustration of the layer-by-layer solution coating method to prepare CNT@TiO_2.

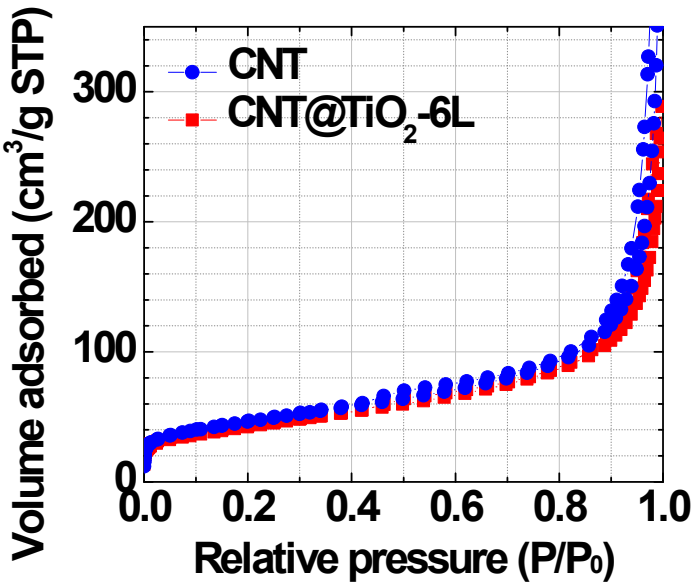

Figure S2. N2 adsorption/desorption isotherms of CNT and CNT@TiO_2.

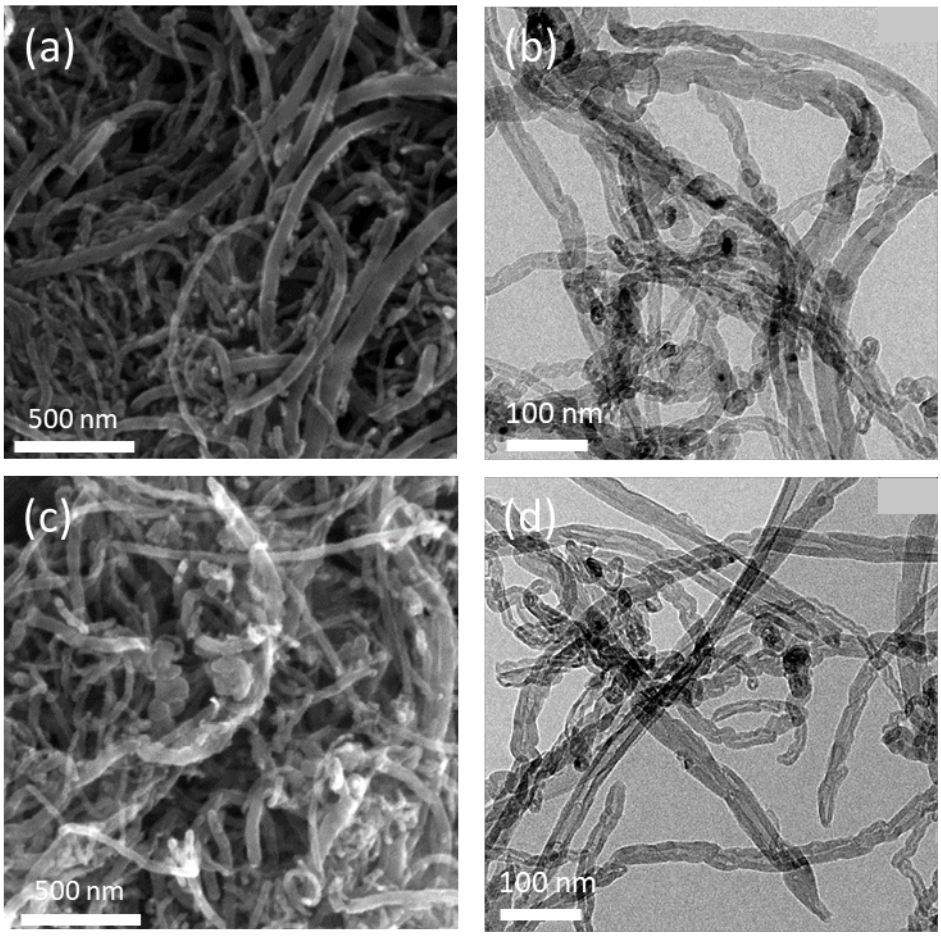

Figure S3. (a) SEM and (b) TEM images of as-purchased multiwall CNTs. (c) SEM and (d) TEM images of acid-treated CNTs.

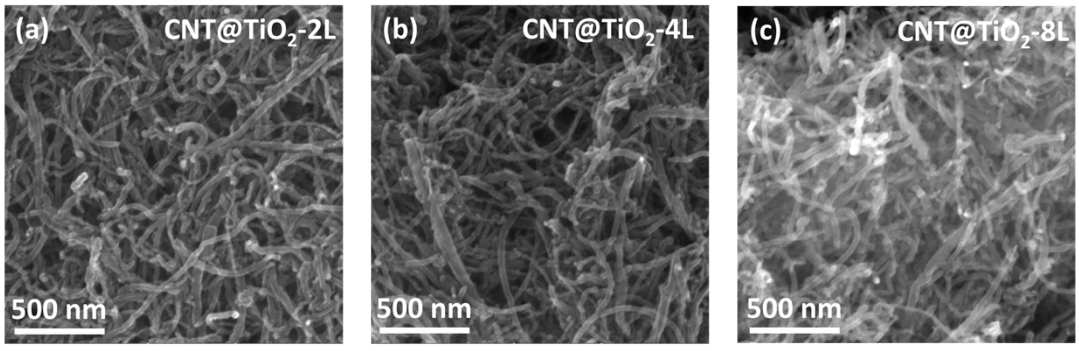

Figure S4. SEM images of (a) CNT@TiO_2-2L, (b) CNT@TiO_2-4L and (c) CNT@TiO_2-8L nanocomposites.

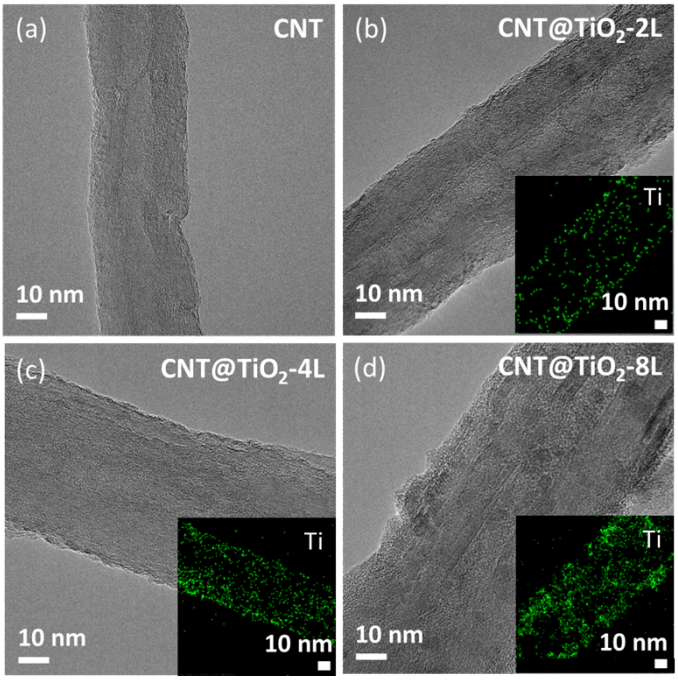

Figure S5. TEM images of (a) CNT, (b) CNT@TiO_2-2L, (c) CNT@TiO_2-4L and (d) CNT@TiO_2-8L nanocomposites. Insets are EDS mapping images for Ti.

Table S1. Titanium (Ti) composition in CNT@TiO_2-nL (n=2, 4, 6, and 8) nanocomposites measured using EDS.

Sample name	Ti (at.%)
CNT@TiO_2-2L	1.1
CNT@TiO_2-4L	3.4
CNT@TiO_2-6L	5.3
CNT@TiO_2-8L	5.5

Table S2. Ir content in Ir/CNT and Ir/CNT@TiO_2-nL (n=2, 4, 6, and 8) nanocomposites measured using ICP-MS.

Sample name	Ir (wt.%)
Ir/CNT	38.8
Ir/CNT@TiO_2-2L	39.2
Ir/CNT@TiO_2-4L	39.4
Ir/CNT@TiO_2-6L	39.3
Ir/CNT@TiO_2-8L	38.6

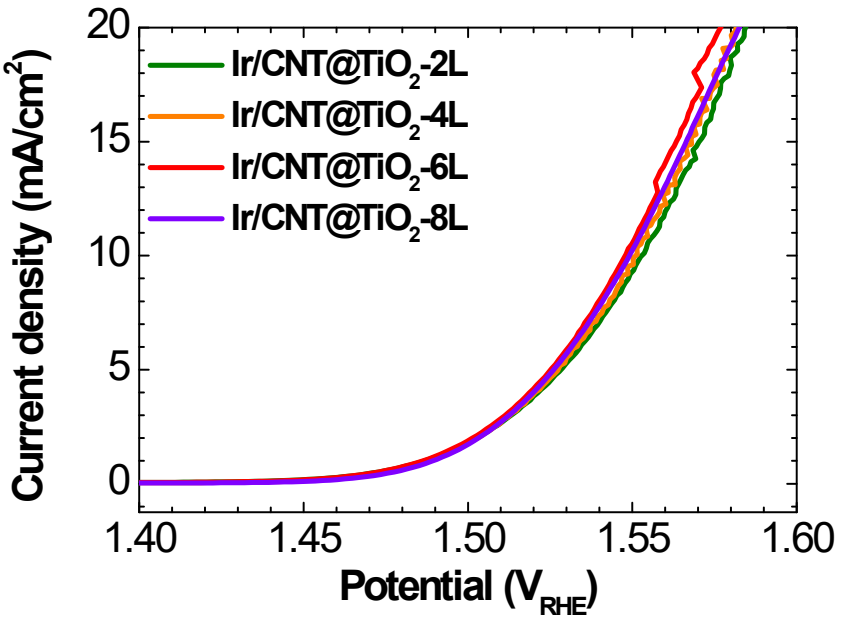

Figure S6. Polarization curve of Ir/CNT@TiO_2-nL (n=2, 4, 6, and 8).

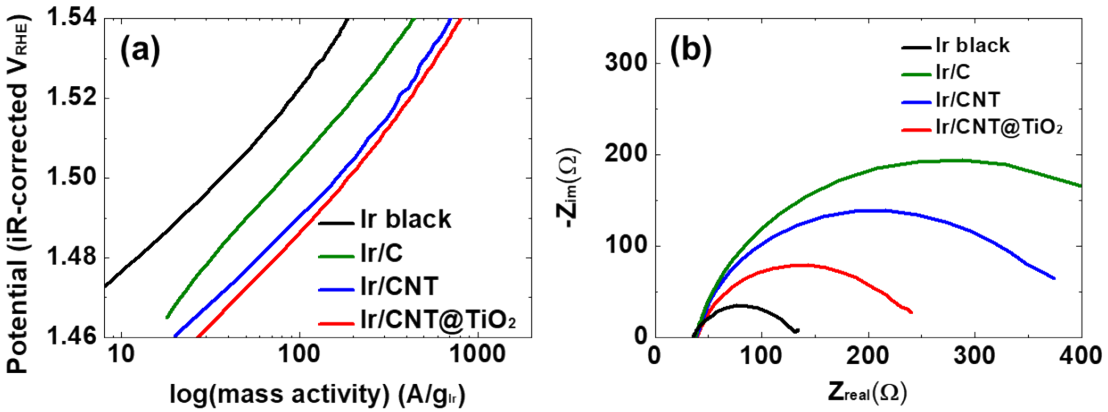

Figure S7. (a) Tafel plots and (b) Nyquist plots for Ir black, Ir/C, Ir/CNT and Ir/CNT@TiO_2.

Table S3. OER mass activity of Ir/CNT@TiO_2 and previously-reported supported Ir-based catalysts measured in acidic media.

Catalyst	Electrolyte	Activity ($A\ g^{-1}_{Ir}$)			Reference
		1.525 V	1.53 V	1.55 V	
Ir/CNT@TiO_2	**0.05 M H_2SO_4**	**496**	**587**	**1055**	**This work**
Ir/ATO-10-NF	**0.05 M H2SO4**			1750	**[1]**
Ir/TiO_2-MoO_x	0.05 M H_2SO_4			573	**[2]**
IrO_X/ATO[b]	0.05 M H_2SO_4		100[a]		**[3]**
IrO_2/TiO_2	0.1 M $HClO_4$	70			**[4]**
IrO_2/TiO_2	0.1 M $HClO_4$	51			**[5]**
IrO_2/$NbTiO_2$	0.1 M $HClO_4$			190[a]	**[6]**
IrO_2/$NbTiO_2$	0.5 M H_2SO_4			160[a]	**[7]**
$IrRuO_X$/$NbTiO_2$	0.5 M H_2SO_4			570[a]	**[8]**

[a] graph-derived values, [b] ATO(Antimony doped tin oxide)

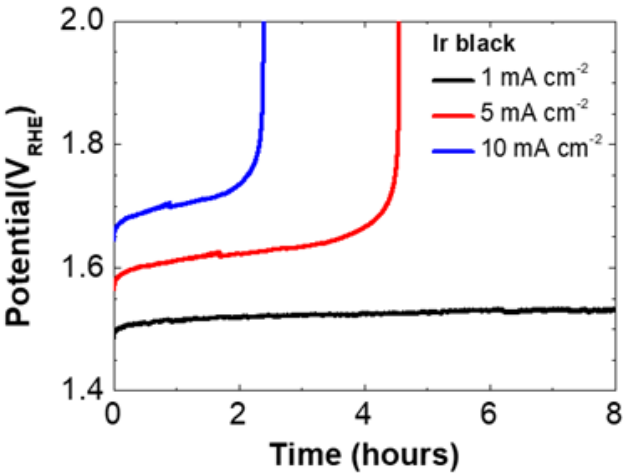

Figure S8. Chronopotentiometry curves of Ir black at 1, 5 and 10 mA cm^{-2}. (Measurement conditions; 37.5 $\mu g_{Ir} \cdot cm^{-2}$, Ar-saturated 0.05 M H_2SO_4 solution, 1600 rpm, 25 °C)

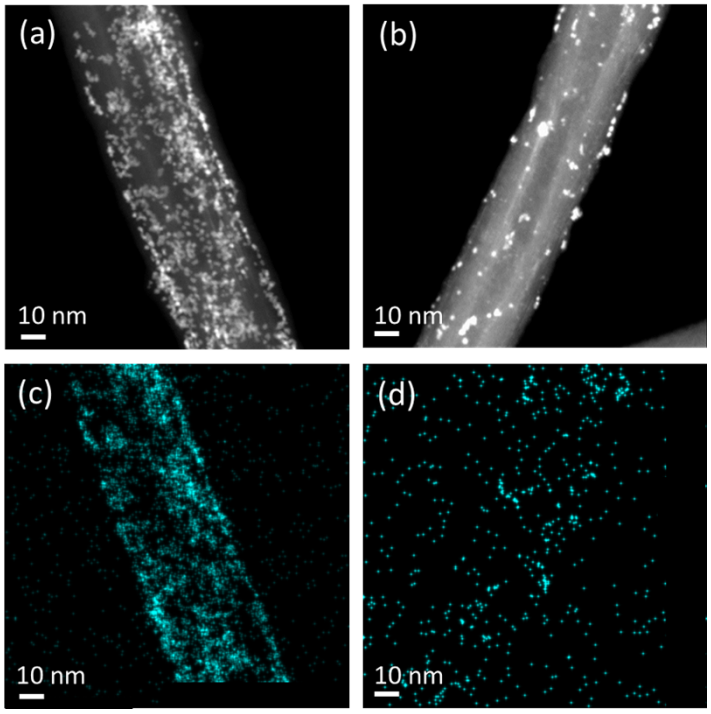

Figure S9. (a), (b) HAADF STEM images of Ir/CNT and (c), (d) EDS elemental mapping

image for Ir (a), (c) before and (b), (d) after the durability test.

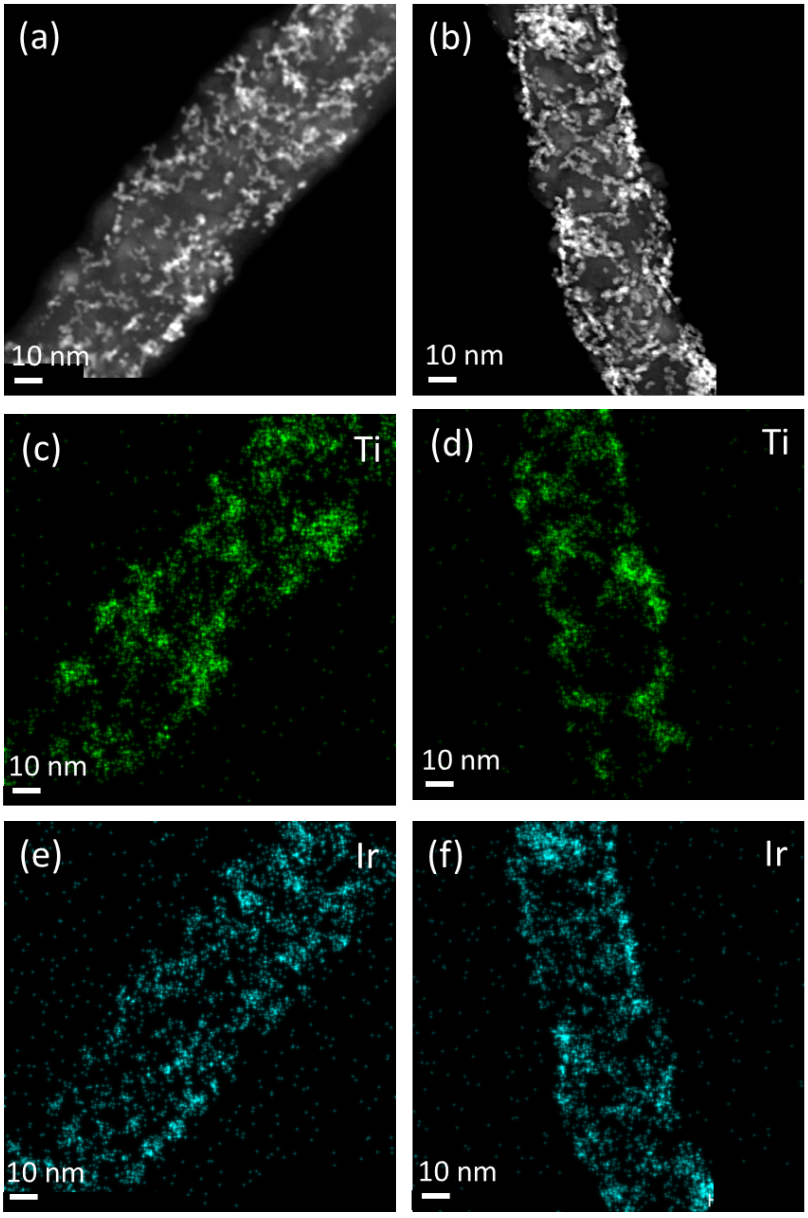

Figure S10. (a), (b) HAADF STEM images of Ir/CNT@TiO_2 and EDS elemental mapping image for (c), (d) Ti and (e), (f) Ir (a), (c), (e) before and (b), (d), (f) after the durability test.

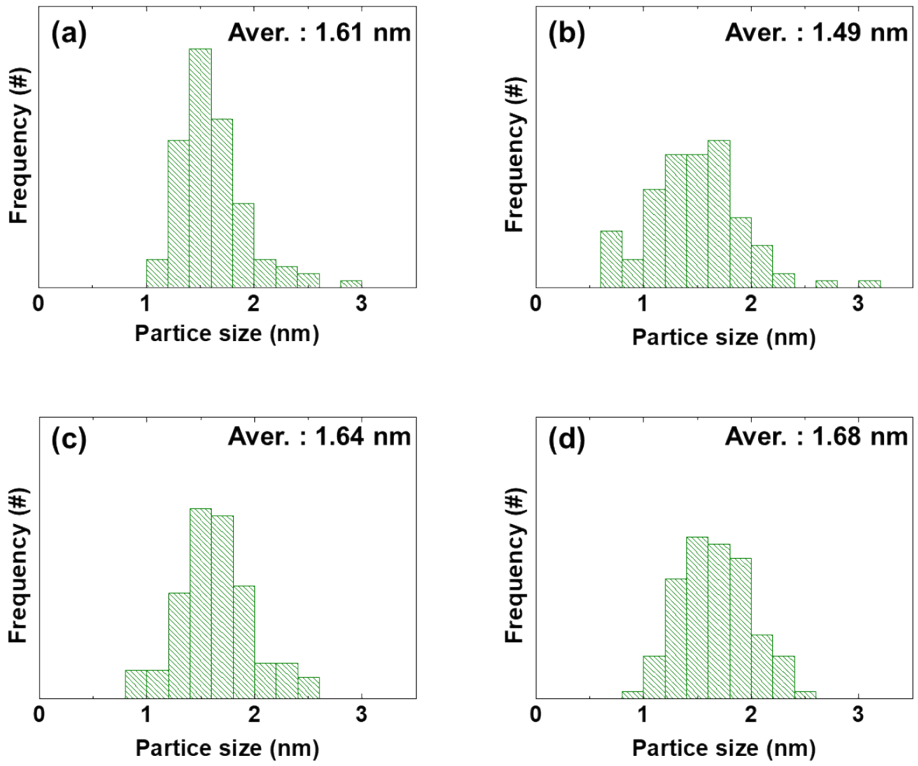

Figure S11. Particle size distribution of Ir nanoparticles of (a),(b) the Ir/CNT and (c),(d) the Ir/CNT@TiO_2 before and after the durability test.

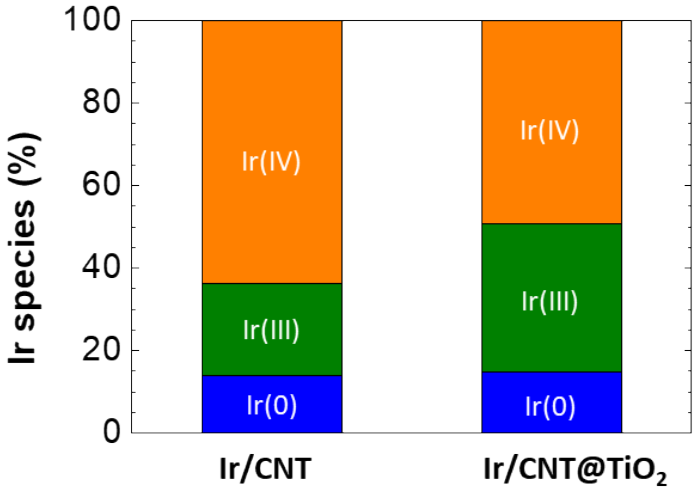

Figure S12. Composition of Ir species for Ir/CNT and Ir/CNT@TiO_2

[1] C. Daiane Ferreira da Silva, F. Claudel, V. Martin, R. Chattot, S. Abbou, K. Kumar, I. Jiménez-Morales, S. Cavaliere, D. Jones, J. Rozière, L. Solà-Hernandez, C. Beauger, M. Faustini, J. Peron, B. Gilles, T. Encinas, L. Piccolo, F.H. Barros de Lima, L. Dubau, F. Maillard, Oxygen Evolution Reaction Activity and Stability Benchmarks for Supported and Unsupported IrOx Electrocatalysts, ACS Catalysis, 11 (2021) 4107-4116.
[2] E.-J. Kim, J. Shin, J. Bak, S.J. Lee, K. hyun Kim, D. Song, J. Roh, Y. Lee, H. Kim, K.-S. Lee, Stabilizing role of Mo in TiO2-MoOx supported Ir catalyst toward oxygen evolution reaction, Applied Catalysis B: Environmental, 280 (2021) 119433.
[3] H.-S. Oh, H.N. Nong, T. Reier, A. Bergmann, M. Gliech, J. Ferreira de Araújo, E. Willinger, R. Schlögl, D. Teschner, P. Strasser, Electrochemical catalyst–support effects and their stabilizing role for IrO x nanoparticle catalysts during the oxygen evolution reaction, Journal of the American Chemical Society, 138 (2016) 12552-12563.
[4] E. Oakton, D. Lebedev, M. Povia, D.F. Abbott, E. Fabbri, A. Fedorov, M. Nachtegaal, C. Copéret, T.J. Schmidt, IrO2-TiO2: A high-surface-area, active, and stable electrocatalyst for the oxygen evolution reaction, Acs Catalysis, 7 (2017) 2346-2352.
[5] C. Van Pham, M. Bühler, J. Knöppel, M. Bierling, D. Seeberger, D. Escalera-López, K.J. Mayrhofer, S. Cherevko, S. Thiele, IrO2 coated TiO2 core-shell microparticles advance performance of low loading proton exchange membrane water electrolyzers, Applied Catalysis B: Environmental, 269 (2020) 118762.
[6] C. Hao, H. Lv, C. Mi, Y. Song, J. Ma, Investigation of mesoporous niobium-doped TiO2 as an oxygen evolution catalyst support in an SPE water electrolyzer, ACS Sustainable Chemistry & Engineering, 4 (2016) 746-756.
[7] W. Hu, S. Chen, Q. Xia, IrO2/Nb–TiO2 electrocatalyst for oxygen evolution reaction in acidic medium, international journal of hydrogen energy, 39 (2014) 6967-6976.
[8] R.V. Genova-Koleva, F. Alcaide, G. Álvarez, P.L. Cabot, H.-J. Grande, M.V. Martínez-Huerta, O. Miguel, Supporting IrO2 and IrRuOx nanoparticles on TiO2 and Nb-doped TiO2 nanotubes as electrocatalysts for the oxygen evolution reaction, Journal of Energy Chemistry, 34 (2019) 227-239.